Flood type specific construction of synthetic design hydrographs

Brunner, Manuela I ; Viviroli, Daniel ; Sikorska, Anna E ; Vannier, Olivier ; Favre, Anne-Catherine ; Seibert, Jan

Abstract: Accurate estimates of flood peaks, corresponding volumes and hydrographs are required to design safe and cost-effective hydraulic structures. In this paper, we propose a statistical approach for the estimation of the design variables peak and volume by constructing synthetic design hydrographs for different flood types such as flash-floods, short-rain floods, long-rain floods, and rain-on-snow floods. Our approach relies on the fitting of probability density functions to observed flood hydrographs of a certain flood type and accounts for the dependence between peak discharge and flood volume. It makes use of the statistical information contained in the data and retains the process information of the flood type. The method was tested based on data from 39 meso-scale catchments in Switzerland and provides catchment specific and flood type specific synthetic design hydrographs for all of these catchments. We demonstrate that flood type specific synthetic design hydrographs are meaningful in flood risk management when combined with knowledge on the seasonality and the frequency of different flood types.

DOI: https://doi.org/10.1002/2016WR019535

Flood type specific construction of synthetic design hydrographs

Manuela I. Brunner[1,2], Daniel Viviroli[1,3], Anna E. Sikorska[1,4], Olivier Vannier[5], Anne-Catherine Favre[2], and Jan Seibert[1,6]

Corresponding author: M. I. Brunner, Department of Geography, University of Zurich, Zurich, Switzerland; Université Grenoble-Alpes, Grenoble INP, LTHE, Grenoble, France (manuela.brunner@geo.uzh.ch)

[1]Department of Geography, University of Zurich, Zurich, Switzerland.

[2] Université Grenoble-Alpes, Grenoble INP, LTHE, Grenoble, France.

[3]belop gmbh, Sarnen, Switzerland.

[4]Department of Hydraulic Engineering, Warsaw University of Life Sciences – SGGW, Warsaw, Poland

[5]Compagnie Nationale du Rhône (CNR), Lyon, France

[6]Department of Earth Sciences, Uppsala University, Uppsala, Sweden.

This article has been accepted for publication and undergone full peer review but has not been through the copyediting, typesetting, pagination and proofreading process which may lead to differences between this version and the Version of Record. Please cite this article as an 'Accepted Article', doi: 10.1002/2016WR019535

Abstract. Accurate estimates of flood peaks, corresponding volumes and hydrographs are required to design safe and cost-effective hydraulic structures. In this paper, we propose a statistical approach for the estimation of the design variables peak and volume by constructing synthetic design hydrographs for different flood types such as flash-floods, short-rain floods, long-rain floods, and rain-on-snow floods. Our approach relies on the fitting of probability density functions to observed flood hydrographs of a certain flood type and accounts for the dependence between peak discharge and flood volume. It makes use of the statistical information contained in the data and retains the process information of the flood type. The method was tested based on data from 39 meso-scale catchments in Switzerland and provides catchment specific and flood type specific synthetic design hydrographs for all of these catchments. We demonstrate that flood type specific synthetic design hydrographs are meaningful in flood risk management when combined with knowledge on the seasonality and the frequency of different flood types.

1. Introduction

Accurate flood estimates are needed for the design of hydraulic structures and for flood risk management. The major quantity of interest in flood estimation is the magnitude of the flood peak corresponding to a specific return period [*Rosbjerg et al.*, 2013]. Flood peaks, however, provide only a limited description of a flood event. For the prevention of flood damage and for designing hydraulic structures, it is also important to know the flood volume and the shape of the flood hydrograph [*Mediero et al.*, 2010]. Design flood hydrographs provide this information for any specified return period and, hence, unite the physical properties of a flood event and statistical information about the event rarity [*Serinaldi and Grimaldi*, 2011]. Design flood hydrographs are hydrographs of a suitable probability and magnitude adopted to ensure the safety of hydraulic structures [*Xiao et al.*, 2009], such as dam spillways, bridges, road culverts, levees, or retention basins. Such hydrographs are also used to estimate sediment loads [*Rickenmann*, 1997], and to draw hazard maps for landuse and urban planning. Design flood hydrographs contain information on several dependent design variables such as peak magnitude, flood volume, and duration, which together determine the severity of a flood. Different flood hydrograph shapes may cause differences in the costs of hydraulic structures and influence flood-control policies and flood management strategies [*Yue et al.*, 2002].

Two approaches are used for design flood estimation, probabilistic and deterministic methods [*Smithers*, 2012; *Rogger et al.*, 2012]. Although these are fundamentally different, they are often confused [*Pilgrim and Cordery*, 1993]. While probabilistic methods are based on the analysis of relatively long flood records, deterministic methods are based on

rainfall data and take into account some catchment processes. The latter are based on the critical assumption [*Viglione et al.*, 2009] that the return period of rainfall and resulting discharge are the same and require the choice of an antecedent soil moisture input [*Pilgrim and Cordery*, 1993; *Rogger et al.*, 2012]. A combination of the two approaches involves the calibration of a rainfall-runoff model [*Boughton and Droop*, 2003; *Pathiraja et al.*, 2012; *Pilgrim and Cordery*, 1993], running it with stochastically generated rainfall to obtain a long flood record, and a subsequent probabilistic analysis [*Rogger et al.*, 2012]. For the design of minor works, such as bridges and culverts, farm dam spillways, and urban drainage systems, where a certain risk of failure is acceptable, a simple method is needed that is easily applicable by designers with little hydrologic expertise, is physically sound, gives reproducible answers [*Pilgrim and Cordery*, 1993], and does not involve the calibration of a continuous simulation model [*Boughton and Droop*, 2003].

In this study, we propose a simple probabilistic method that is based on observed runoff data only and thus does not require the use of any rainfall-runoff model. The method estimates peak magnitude and flood volume using frequency analysis and uses a prescribed mathematical function to model the flood shape. The combination of the flood variable estimates and the flood shape results in a *synthetic* design hydrograph (SDH).

Several methods have been proposed to derive unit hydrographs that can serve as the basis for design flood hydrographs. *Yue et al.* [2002] gave an overview on existing unit hydrograph methods and grouped them into four types: traditional unit hydrograph (TUH), synthetic unit hydrograph (SUH), typical hydrograph (TH), and statistical methods (SM). The TUH of a watershed is defined as the direct runoff hydrograph resulting from a unit volume of excess rainfall of constant intensity and uniformly distributed over the drainage

area [*Ramirez*, 2000]. The SUH is defined on the basis of catchment characteristics or expert knowledge and often assumes a triangular shape of the hydrograph, whereas the TH selects a typical flood hydrograph (usually the flood hydrograph with the highest peak discharge or flood volume) from sampled flood series [*Yue et al.*, 2002]. *Bhunya et al.* [2007] stated that the statistical methods (SM), which are based on probability density functions (PDFs), are more suitable to derive unit hydrographs than traditional methods because the area under the curve is guaranteed to be equal to one and can therefore be used as the basis for a design flood hydrograph. Further, probability density functions are quite flexible and can take various shapes. *Yue et al.* [2002] proposed a method that employs the PDF of the Beta distribution, which allows a unit hydrograph to be represented with different shape types, due to the flexibility of the Beta distribution, that can be used as the basis for a design flood hydrograph. *Nadarajah* [2007] used nine additional PDFs to derive the basis for a design flood hydrograph, namely, the Lognormal, inverse Gamma, Kumaraswamy, Two-sided-power, Pareto, inverse Gaussian, F, Weibull, and Fréchet density functions. He provided estimates of the PDFs' parameters in terms of the time to peak, peak discharge, and the duration of the direct runoff hydrograph, also called the time base [*Ramirez*, 2000]. However, neither *Yue et al.* [2002] nor *Nadarajah* [2007] provide a tool to move from the dimensionless shape of the design hydrograph to an actual design flood hydrograph. *Serinaldi and Grimaldi* [2011] overcame this deficiency by linking the dimensionless hydrograph in the form of a Beta density ($f(t)$) with the design variables flood volume V_T and duration D_T corresponding to a fixed return period T to obtain a SDH called $Q_T(t)$, expressed as

$$Q_T(t) = f(t)V_T/D_T. \quad (1)$$

In this study, we make use of the concepts outlined above but implement a joint design event which takes account of the dependence between peak discharge and flood volume to upscale the dimensionless hydrograph shape to a synthetic design hydrograph for a given return period T.

The SDHs do not contain any information about the hydrological processes underlying the design event. However, additional insight into a catchment's behavior could potentially be gained when looking at design hydrographs constructed for different flood types such as flash floods, short-rain floods, long-rain floods, or rain-on-snow floods which have different probabilities of occurrence. Such a flood type specific analysis is also advantageous from a statistical point of view because we avoid mixing events caused by different processes and can better justify the assumption commonly made in flood frequency analysis that the variables (peak discharge and flood volume) are independent and identically distributed (i.i.d.) random variables [*Klemes*, 2000; *Merz et al.*, 2014] even though they are usually jointly dependent [*Serinaldi and Kilsby*, 2013]. Besides containing the physical properties and the statistical information, such flood type specific design hydrographs indicate what types of floods might require special attention in flood risk management.

Here, we go one step further than previous studies by not only constructing catchment specific SDHs, which sum up the overall flood behavior of a catchment, but also constructing flood type specific SDHs. This is done by complementing the statistical nature of the method with process based knowledge stored in the flood event data. It has been pointed out by *Merz and Blöschl* [2008a] that expanding information beyond the flood

sample is very useful for accurately estimating flood frequencies. Knowledge on the characteristics of a flood reflected by the flood type can lead to a better understanding of floods and might improve their prediction accuracy. *Sikorska et al.* [2015] suggested that the classification of floods at the event level along with the information of their frequency may support flood risk management because the effects of flooding on the inundated area will alter depending on the specific flood behavior. Therefore, we propose a way of deriving flood type specific SDHs for four frequently observed and potentially hazardous flood types, *i.e.* flash floods, short-rain floods, long-rain floods, and rain-on-snow floods, using a dimensionless hydrograph represented by a probability density function and design variable quantiles estimated for a specified return period using a joint frequency analysis. The method takes into account that different types of floods are characterized by different dependence structures between peak discharges and flood volumes [*Gaal et al.*, 2015; *Grimaldi et al.*, 2016; *Szolgay et al.*, 2015].

2. Data

The proposed method has been developed and tested using runoff, precipitation, and temperature data from a representative set of 39 meso-scale (catchment area 20-1700 km^2) catchments in Switzerland (see Figure 1 and Table 3 in the Appendix for a complete list). The selected catchments have hourly flow data series, which is crucial for characterizing the shape of the flood hydrographs, with a length of 17 to 53 years, with 50% of the catchments having a record length of 30 to 40 years. We selected catchments only with natural flow conditions neither altered through hydropower plants nor lake regulation or water transfers, to avoid hydrograph shapes modified by direct human impacts. We excluded highly glacierized catchments because unimpaired flow records are scarce for

these. The characteristics of the 39 study catchments selected are summarized in Table 1. The median catchment size is 119 km^2, and there are only four large catchments with a size of more than 500 km^2. Most measurement stations lie below 750 m.a.s.l. and only four stations are located at altitudes higher than 1000 m.a.s.l. Most catchments have a mean elevation lower than 1500 m.a.s.l. meaning that mountainous catchments are scarce [*Viviroli and Weingartner*, 2004]. However, there are two partly glacierized catchments in the set with a degree of glaciation of 6.7% and 14.2% respectively. The median of the maximal observed peak discharges in the study catchments is 122 m^3/s, while the median of the maximal specific observed peak discharges (discharge per unit area) is 947 $l/(s{\cdot}km^2)$. The median of the maximal observed flood volumes is 1918 m^3, although, there are catchments with significantly higher maximal flood volumes. The median of the maximal specific flood volume (volume per unit area) is 4197 $10^3{\cdot}$ m^3/km^2.

We selected three catchments having similar mean elevation (between 650 and 800 m.a.s.l.) to represent three catchment size classes (small, medium, and large) as examples to show more detailed results. These illustration catchments are the Langete at Huttwil (60 km^2), the Mentue at Yvonand (105 km^2), and the Birs at Münchenstein (911 km^2) (see green catchments in Figure 1).

3. Methods

The construction of flood type specific SDHs relies on the fitting of probability density functions to observed flood hydrographs of a certain flood type and takes account of the dependence between the design variables peak discharge and flood volume. The different steps involved in constructing flood type specific SDHs are displayed in Figure 2 and are described in more detail in the following paragraphs whose numbers correspond to

the numbers used in Figure 2. The proposed method can either be applied to construct a catchment specific SDH without a differentiation between flood types or to construct flood type specific SDHs.

3.1. Flood sampling

The SDH construction method is based only on observed runoff data. Thus, historical flood event hydrographs were selected in the 39 representative Swiss catchments described in Section 2 (see Figure 1 and Table 3). To sample flood events, we used a peak-over-threshold (POT) approach based on the procedure proposed by *Lang et al.* [1999] which is superior to annual maxima sampling [*Tanaka and Takara*, 2002] because it allows for a more rational selection of events to be considered as floods than annual maxima sampling [*Lang et al.*, 1999]. The threshold for the peak discharge was chosen iteratively to fulfill a target condition of four events per year on average which is a trade-off between maximizing the information content in the sample and keeping the assumption of independence between events. The independence between successive events was additionally ensured by prescribing a minimum time interval of 72 hours between them. However, most of the sampled events were separated by at least five days. According to extreme value theory, POT values follow a generalized Pareto distribution (GPD) [*Coles*, 2001]. Therefore, we used a GPD to fit the peak discharge values. For each of these events, sampled according to the flood peaks, the flood volume was determined over a fixed event window of 72 hours. The flood volumes were not selected as peak over threshold values, and did not necessarily represent annual maxima. Therefore, we tested several statistical distributions to fit the distribution of the flood volumes. The generalized extreme value distribution (GEV) was found to fit the data best. The GPD model has three continuous parameters:

a location parameter μ in $\mathbb{R}$, a scale parameter $\sigma > 0$, and a shape parameter ξ in $\mathbb{R}$. It is defined as

$$F_X(x) = 1 - \left\{1 + \xi\Big(\frac{x-\mu}{\sigma}\Big)\right\}^{-\frac{1}{\xi}} \qquad \xi \neq 0, \tag{2}$$

where x is larger than a threshold μ.

On the other hand, the GEV uses the same parameters and is expressed as

$$F_Y(y) = \exp\left[-\left\{1 + \xi\Big(\frac{y-\mu}{\sigma}\Big)\right\}^{-\frac{1}{\xi}}\right] \qquad \xi \neq 0 \tag{3}$$

with domain $1 + \xi\left(\frac{y-\mu}{\sigma}\right) > 0$ for $\xi \neq 0$.

The goodness-of-fit of the GPD to the peak discharges and the GEV to the flood volumes was checked visually using *qq*-plots and *pp*-plots and tested using the Kolmogorov-Smirnov and the Anderson-Darling tests, plus the upper-tail Anderson-Darling test [*Chernobai et al.*, 2015], which gives a higher weight to the fit in the upper tail (of special interest here) than to the remaining parts of the distribution. The upper-tail Anderson-Darling test confirmed the visual impression that the GPD fits the peak discharges and the GEV distribution fits the flood volumes well.

3.2. Classification

To construct flood type specific SDHs, the data set needs to be divided into subsets of different flood types. Therefore, each sampled flood event was attributed to a specific flood type according to its triggering mechanism using a flood classification scheme proposed by *Merz and Blöschl* [2003], complemented by *Diezig and Weingartner* [2007], and extended by *Sikorska et al.* [2015]. The classification scheme applied is based on successive binary splittings of the set of flood events into smaller groups of flood events according

to predefined decision attributes and results in the assignment of each flood event to one of six flood types [*Sikorska et al.*, 2015]. The following six flood types, having different causative mechanisms, are considered:

1. Flash floods (FF) with short but very intense rainfall, usually lasting less than half a day;

2. Short-rain floods (SRF) with rainfall usually lasting no longer than one day;

3. Long-rain floods (LRF) with rainfall lasting several days or even weeks;

4. Rain-on-snow floods (RoSF) with rainfall falling on snow, which initiates its melting;

5. Snowmelt floods (SMF) caused by a melting of a snow cover with no or insignificant rainfall;

6. Glacier-melt floods (GMF) caused by glacier melting with no or insignificant rainfall.

All these flood types show a specific behavior in terms of spatial and temporal characteristics. This makes it possible to distinguish them based on a set of pre-defined, flood-specific indices. As proposed by *Sikorska et al.* [2015], we used the following eight indices to attribute the observed flood events to one of the six flood types: timing of the flood within the year, precipitation amount, precipitation duration, precipitation intensity, glacier cover, snow cover, snowmelt, and catchment wetness. The first four indices were computed on the basis of runoff and precipitation data as in *Sikorska et al.* [2015]. *Sikorska et al.* [2015] used the conceptual hydrological model HBV [*Seibert*, 1999] to compute glacier and snow cover, snowmelt, and catchment wetness. Here, we computed glacier cover from land cover maps, applied a simple degree-day model [*Schreider et al.*, 1997] with a fixed degree-day factor (1.5 mm/degree-day) to compute the snow cover and the snowmelt, and defined the catchment wetness via the current precipitation index (CPI)

[*Smakhtin and Masse*, 2000] (using a daily recession coefficient of 0.9). We tested both the crisp and the fuzzy approaches proposed by *Sikorska et al.* [2015], which led to approximately the same classification results when comparing the result from the crisp decision tree to the dominant flood type obtained with the fuzzy tree. Therefore, the decision attributes were defined as sharp thresholds to attribute exactly one flood type to each event which is facilitating computations in the construction of flood type specific SDHs. The thresholds for some indices were slightly modified from *Sikorska et al.* [2015]: The threshold for snow cover was set to a snow water equivalent of 1 mm to distinguish between the existence and non-existence of snow cover and the threshold for the catchment wetness was set to 90% of the mean of the catchment's CPI.

Knowing all eight indices for each sampled flood event, we were able to attribute each flood event to one of the six flood types introduced above by following a decision tree with sharp thresholds. For a detailed overview of the classification scheme employed, we refer to *Sikorska et al.* [2015].

An objective validation of the flood classification process is not possible because there are no true classes [*Merz and Blöschl*, 2003]. Instead, the observed hydrographs were inspected visually and compared to the class assignments. This comparison showed that the classification procedure results in a reasonable subdivision of events into six flood types. As pointed out by *Merz and Blöschl* [2003], such an automated classification procedure is very useful in the flood frequency context because a large number of events can be classified in a limited amount of time.

The most often observed flood types in the 39 study catchments were SRFs followed by FFs, LRFs, and RoSFs (Figure 3). SMFs and GMFs were relatively rare because there

are only a few mountainous catchments in the dataset. While some of the flood types such as FFs, RoSFs, and SMFs show a high seasonality, other flood types such as SRFs and LRFs occur in all seasons. FFs mainly occur in summer or autumn, RoSFs mainly in winter and spring, and SMFs in winter and spring. The number of events observed per flood type varied between the different catchments. The number of FFs, LRFs, and RoSFs varied between less than 10 and around 55 events, while the number of SRFs lay between 33 and 86 events (Table 2).

In the following, we focus on the four flood types FFs, SRFs, LRFs, and RoSFs because the number of SMF and GMF events was too low to build a large enough sample to estimate SDHs. Furthermore, snowmelt floods were shown to have small flood peaks [*Merz and Blöschl*, 2003] and are therefore less relevant for flood management than the four flood types analyzed in detail.

3.3. Baseflow separation

The SDH approach describes only the quick flow component of the event hydrograph originating from a precipitation event and does not consider the baseflow component. Thus, it is necessary to distinguish between the baseflow and the quick runoff components to analyze the statistical properties of flood hydrographs [*Yue et al.*, 2002]. In this study, we applied a recursive digital filter [*Eckhardt*, 2005] whose two parameters need to be estimated for each catchment. This method allows for the separation of the baseflow from the quick flow, is easily applicable to a wide variety of catchments, and provides reliable results in an objective way [*Serinaldi and Grimaldi*, 2011; *Gonzales et al.*, 2009]. A visual assessment showed that the method produces smooth and plausible baseflow curves. In a later step, we added a representative baseflow to the constructed SDH to obtain the total

hydrograph. Thus, we computed a baseflow index (I_{BF}), which is the ratio between the volume of baseflow divided by the volume of total streamflow [*Smakhtin*, 2001] for each event as proposed by *Meyer et al.* [2011]. This allowed us to compute a mean baseflow index for each flood type and a catchment specific baseflow index.

3.4. Normalization

The quick flow component of the hydrographs was normalized so that both the base width and the volume of the modified hydrographs were equal to one. This was done by dividing the base width of each flood hydrograph by its duration D and then dividing the ordinate of each hydrograph by the mean runoff given by the ratio of flood volume V and duration D (V/D).

3.5. Identification of a representative normalized hydrograph

A normalized hydrograph, which is representative of a catchment's flood behavior, needs to be chosen for the non-flood-specific construction of an SDH. In addition, one representative, normalized hydrograph per flood type needs to be defined. A representative normalized hydrograph (RNH) was defined as the median normalized hydrograph of the corresponding event set (one set for all flood events and one separate set for each flood type). We chose the median normalized hydrograph instead of the mean normalized hydrograph because it refers to a real observed event, which is not necessarily the case for the mean of the normalized hydrographs.

The median hydrograph was defined using a notion of depth for functional data [*Ramsay and Silverman*, 2002]. The concept of data depth aims at measuring the centrality of a given curve (in our case, the hydrographs) within a group of curves and can be used

to define the ranks of functional data [*Fraiman and Muniz*, 2001] and therewith robust estimators of a location parameter such as the median or the trimmed mean. Several data depths proposed in the literature are suitable for functional data, among them, the depth proposed by *Fraiman and Muniz* [2001], the h-mode depth, the random-projection depth [*Fraiman and Muniz*, 2001], or the band depth [*López-Pintado and Romo*, 2009]. We used the *h-mode* depth to order the hydrographs in the sample since it was found to perform best if one is interested in finding the median curve within a set of curves [*Cuevas et al.*, 2007].

3.6. Fitting of a probability density function

The shape of a normalized hydrograph can be fitted by a probability density function (PDF) because both the area under the normalized hydrograph and the area under the PDF are equal to one and because probability density functions can take various shapes. *Nadarajah* [2007] and *Rai et al.* [2009] derived expressions for the unknown parameters of several density functions in terms of the time to peak (t_p), the peak discharge (q_p) and the time base (t_B) of the RNH. If the distribution has a finite support, its upper end point can be taken to correspond to the time base t_B. The time to peak t_p can be defined by the value of x that maximizes the PDF $f(x)$ and the peak discharge q_p as the value of $f(x)$ at t_p. To select the most suitable density, eight different commonly used PDFs were fitted to all of the RNHs in the 39 study catchments: Normal, Lognormal, Fréchet, Weibull, Logistic, Gamma, inverse Gamma, and Beta [*Nadarajah*, 2007; *Serinaldi and Grimaldi*, 2011]. The two parameters (characterizing location and scale or scale and shape) of the distributions were estimated based on the three characteristics t_B, t_p, and q_p so that the PDFs approximate the shape of the RNHs as well as possible. The goodness-

of-fit of each PDF to the RNH was assessed by comparing the mean of the four following performance criteria for the different density functions: bounded Nash-Sutcliffe efficiency [*Mathevet et al.*, 2006], volumetric efficiency, Kling-Gupta efficiency [*Gupta et al.*, 2009], and Spearman's correlation coefficient. The Lognormal density function modelled the RNHs best, closely followed by the inverse Gamma and Fréchet densities. We therefore used the Lognormal density function to model the RNHs of the different flood types and the catchment specific RNH. The modelling of the flood specific RNH was done with only a minimum of five events in the different flood type specific datasets to ensure reliable parameter estimates. This means that we could produce SDHs only for floods of those types for which we had more than five observed events in a catchment. In practice, this meant that a specific SDH for one of the flood types could not be produced in 18% of the catchments.

The fitting of PDFs to an RNH to determine the dimensionless shape of the design hydrograph proved to be effective and allows for an upscaling of the dimensionless shape to an SDH using design variable quantiles. However, the fitting of PDFs can pose a problem in the case of catchments with events with more than one peak [*Yue et al.*, 2002]. There, a fitting of the hydrograph with a PDF can result in large volume differences. One could fit mixture distributions (*i.e.* a combination of distributions) [*Mengersen et al.*, 2011] to hydrographs with multiple peaks to reduce such differences in volume but parameters of the mixture would be difficult to estimate with the sample size at hand and because of numerous interacting parameters, which would lead to identifiability problems.

3.7. Dependence modelling

The dependence between peak discharge (Q_{max}) and flood volume (V) was assessed graphically using Chi-plots and K-plots and tested numerically by computing two rank correlation coefficients, Kendall's tau and Spearman's rho [*Genest and Favre*, 2007]. The bivariate distribution of peak discharges and flood volumes was expressed in the form of a copula model which, in contrast to a classical bivariate distribution, allows for modelling the dependence between the two variables independently of the choice of their marginal distributions [*Joe*, 2014]. Copulas are multivariate distribution functions whose marginal distributions are uniform. In contrast to standard multivariate distributions, copula models thus allow the variables to be characterized by different marginal distributions. The advantages of this approach are that the selection of an appropriate model for the dependence between variables, represented by the copula, can then proceed independently from the choice of the marginal distributions and that a wide selection of copula families is available to model different dependence structures [*Genest and Favre*, 2007]. For a more thorough introduction to copulas, we refer the reader to the textbooks of *Nelsen* [2005] or *Joe* [2014] or the review paper by *Genest and Favre* [2007]. The location, scale, and shape parameters of the marginal distributions GEV (Equation 3) for the flood volumes and GPD (Equation 2) for the peak discharges were estimated using the maximum likelihood method [*Coles*, 2001]. The appropriate copula to model these marginal distributions was chosen amongst eight copula models: five copula models of the Archimedean copula family (Gumbel, Clayton, Joe, Frank, Ali-Mikhail-Haq (AMH)), two copula models of the elliptical copula family (Student and Normal copula), and the independence copula. They were fitted to the pseudo-observations (which are deduced from the ranks of the obser-

vations) using maximum pseudo-likelihood estimation, which was shown to perform best under known margins [*Hofert et al.*, 2012]. After the fitting, they were tested using both graphical approaches and a goodness-of-fit test based on the Cramér-von Mises statistic [*Genest and Favre*, 2007]. A p-value for the Cramér-von Mises statistic of each copula was estimated using a statistical bootstrap procedure [*Genest et al.*, 2009]. The copula models which were not rejected at the $\alpha = 0.05$ significance level in most of our study catchments were the Joe and the Gumbel copula. Between these two copulas, we chose the Joe copula for further analysis because it was rejected in only 13% of the catchments. The Joe copula is described by

$$C(u,v) = 1 - \left[(1-u)^\theta + (1-v)^\theta - (1-u)^\theta(1-v)^\theta\right]^{\frac{1}{\theta}}, \tag{4}$$

where θ is the copula parameter, $u = F_X(x)$ and $v = F_Y(y)$ are uniformly distributed between 0 and 1, and their dependence is modeled by the copula C.

The Joe copula is very flexible and can represent the bivariate distributions of all flood types. In addition, it is able to consider tail dependence [*Heffernan*, 2000] which is crucial when moving towards higher return periods. The form of the dependence represented by the copula model was used for all flood types while the copula parameter θ, expressing the strength of dependence, was estimated for each flood type separately. While an individual treatment of flood types can be beneficial when modelling the dependence between peak discharges and flood volumes [*Szolgay et al.*, 2015; *Gaal et al.*, 2015], here, testing the suitability of other copula types for the different flood types separately was not possible since the sample at hand was too small for such an analysis [*Genest et al.*, 2009]. *Grimaldi et al.* [2016] recently suggested that the actual sample size could be increased by merging

the available data with other observations collected in hydrologically similar catchments. Merging the flood type specific datasets from similar catchments might allow for the estimation of the form of the copula for the individual flood types. Still, the Joe copula seems to be able to model the dependence between peak discharges and volumes well for different flood types by choosing different copula parameters for the different dependence intensities.

3.8. Choice of a return period definition

Before estimating the design variables, a value for the return period or recurrence interval T needs to be chosen (*e.g.* 20 years, 50 years, or 100 years). Since we deal with not only one but two non-independent variables, peak discharge and flood volume, we also need to choose a definition for the return period in addition to the value for T. In a multivariate framework, a specific return period definition needs to be chosen depending on the problem at hand [*Serinaldi*, 2015a]. Several ways of defining a multivariate return period have been proposed in the literature, which all rely on different probability concepts. Definitions use the conditional probability, the joint probability (OR or AND), or can be based on Kendall's distribution or survival function. For a comprehensive overview on the topic please refer to *Brunner et al.* [2016] and the references cited therein. Assuming that the dependence between peak discharges and flood volumes is important for a potential application of this method, we used the joint OR return period definition which takes into account the dependence between Q_{max} and V by relying on the probability of either Q_{max} or V exceeding given thresholds. The joint OR return period is defined as

$$T(x,y) = \frac{\mu}{\Pr[X > x \vee Y > y]} = \frac{\mu}{1 - F_X(x) - F_Y(y) + F_{XY}(x,y)} = \frac{\mu}{1 - C(u,v)}, \quad (5)$$

where X and Y are random variables, C is a copula, x and y are given thresholds, μ is the inter-arrival time between two successive events $u = F_X(x)$ and $v = F_Y(y)$, and F_X, F_Y, and F_{XY} are the marginal and joint distribution functions of the random variables respectively.

We based our analysis on a joint return period definition but other return period definitions could also be used. As was pointed out in *Serinaldi* [2015a] and *Brunner et al.* [2016], the choice of the return period definition to be used to estimate design variable quantiles should be chosen according to the problem at hand in practice.

3.9. Estimation of Q_T and V_T

The pair of design variable quantiles, Q_{max} and V, associated with a defined joint OR return period T was estimated using the marginal distributions of the variables and the Joe copula to model their dependence. For the marginal distributions, we assumed a GEV distribution for the flood volumes and a GPD for the peak discharges. We retained the pairs $(F_X(x), F_Y(y))$ that were located along the probability level t corresponding to the given return period T such that $1 - t = 1 - C(u, v)$. All the pairs (u, v) that are at the same probability level t are eligible because they correspond to the return period T. The design variable pairs were then calculated by inverting their marginal distributions F_X (for peak discharges) and F_Y (for flood volumes)

$$Q_{maxT} = F_X^{-1}(u) \tag{6}$$

and

$$V_T = F_Y^{-1}(v). \tag{7}$$

There is no unique solution of the design variables associated with the joint OR return period T. Instead, all the possible solutions are located along the return period level, which is a curve on a bi-dimensional graph with Q_{max} and V as coordinates. We chose the design realization on this isoline that maximized the likelihood to construct the SDH [*Salvadori et al.*, 2011]. A detailed description of the estimation procedure can be found in *Brunner et al.* [2016].

3.10. Computation of D_T

We restricted our analysis to the bivariate case not considering the dependence between flood volume and duration because we consider the duration of an event to be of less interest for practitioners than peak discharge and flood volume. Therefore, the third design variable, the duration D_T, follows from the estimates of Q_T and V_T and is defined as $D_T = f(t_p) \cdot V_T/Q_T$, where $f(t_p)$ is the Lognormal density at the time of peak t_p. This means that the duration D_T cannot be determined independently but results from the design variable quantiles Q_T and V_T [*Serinaldi and Grimaldi*, 2011]. Considering the dependence between event duration and flood volume would move us to a trivariate setting, where inference is computationally more challenging [*Hofert et al.*, 2012], which requires considerably more data for reliable estimation than the bivariate case [*Klein et al.*,

2010], and which is limited by the range of the dependence structures the copula chosen can handle [*Hao and Singh*, 2016].

3.11. SDH construction

An SDH can be constructed for each flood type and over all flood types using the Lognormal distribution fitted to the respective RNH and the estimates for V_T and D_T according to Equation 1. The baseflow, which was removed from total flow in Step 3 of the procedure, has to be readded to the SDH to receive total flow instead of quick flow. The baseflow to be added is determined by the flood type specific baseflow index computed in Step 3 of the procedure. This index is multiplied with the runoff at each time step to obtain a baseflow proportional to the quick flow. Hence, the construction of the final SDH requires knowledge of ten parameters: baseflow index, location and scale parameter of the Lognormal distribution, a location, scale, and shape parameter for the two marginal distributions of the peak discharges and the flood volumes as well as the parameter θ of the Joe copula.

4. Results

4.1. SDH parameters per flood type

The parameters of the SDHs were estimated for the 39 study catchments in two ways: based on the whole sample of events and using only the flood type specific event sets. The results show that different flood types are characterized by different SDH parameters (Figure 4). The parameters for the baseflow index, dependence (θ), and the location and scale of the Lognormal PDF show some dependence on the flood type while the parameters of the marginal distributions of the peak discharges and flood volumes do not

show any dependene on the flood type. The baseflow index I_{BF} (Figure 4a) is generally highest for FFs, followed by SRFs and RoSFs. LRFs possess the lowest baseflow indices. Even though the medians of the flood type specific baseflow indices differ, their variability is quite large. Concerning the copula parameter, FFs and SRFs are characterized by a low dependence between peak discharges and volumes and show thus small values of θ (Figure 4b). On the contrary, LRFs are characterized by a larger dependence between peak discharges and volumes and have higher θ values. The θ values of the RoSFs are in between those of the shorter and longer events. The location parameter of the Lognormal distribution increases with the event duration from FFs over SRFs to LRFs (Figure 4c). The scale parameter is highest for SRFs and lowest for RoSFs (Figure 4d).

4.2. Flood type specific SDHs

Based on the SDH parameters estimated per flood type, flood type specific SDHs were derived. Figure 5 displays the flood type specific SDHs for the three example catchments Langete at Huttwil (a), Mentue at Yvonand (b), and Birs at Münchenstein (c) together with an overall SDH which is not flood type specific. In the smallest catchment Langete at Huttwil, the magnitude of the peak discharges of the SDHs decreases with the duration of the precipitation event causing the flood, meaning that FFs have high peak discharges while LRFs have low peak discharges. In the medium sized catchment Mentue at Yvonand, the SRFs cause the highest peaks and are, together with the RoSFs, responsible for the highest volumes. In the largest catchment Birs at Münchenstein, SRFs, which are the most frequently observed event type, are characterized by high peak discharges and volumes. There is a tendency of floods being more attenuated in larger catchments than in small catchments.

Figure 6 shows the two design variables peak discharge [l/(s·km^2)] (a) and volume [10^3· m^3/km^2] (b) per unit area for three different catchment size groups, namely, small catchments (20-75 km^2), medium sized catchments (76-300 km^2), and large catchments (301-1700 km^2), for the different flood types. When looking at catchments of all sizes, there are only small differences between specific peak discharges (peak discharge per unit area) for different flood types. However, there is a visible difference between the peaks of different flood types within the groups of catchments of similar size. In small catchments, shorter events such as FFs and SRFs have generally higher specific peak discharge than longer events such as LRFs and RoSFs. The contrary can be observed in medium sized and large catchments, where LRFs and RoSFs are generally characterized by higher specific peak discharges than shorter events such as FFs and SRFs. For the specific flood volumes, we identify a similar pattern independently of the catchment size: LRFs show higher volumes than RoSFs, and clearly higher volumes than SRFs and FFs.

4.3. Flood type specific SDHs for different return periods

Figure 7 shows flood type specific SDHs (a) and flood type specific design variable quantiles (b) for three different return periods, commonly used in engineering practice, $T = 20$, $T = 50$, and $T = 100$ for the catchment Mentue at Yvonand. While the SDHs for different return levels have different peak discharges and flood volumes for most of the flood types (SRFs, LRFs, RoSFs, all types combined), the SDHs do differ only slightly for the FFs. The behavior of the different flood types for different return periods can be explained by their bivariate distribution of peak discharges and flood volumes (Figure 7c). The distribution of SRFs and of all types combined allows for both high peak discharge values and high flood volume values. The distributions of LRFs and RoSFs allow for

high volume values but are bounded for the peak discharge values. The distribution of FFs is bounded in both directions. The link between different shapes of the bivariate distribution and the differences in SDHs for different return levels is confirmed in the other study catchments. However, the intensity of the dependence of the bivariate distributions of different flood types varies from catchment to catchment.

5. Discussion

5.1. SDH parameters per flood type

Different flood types were characterized by different SDH parameters. First, the baseflow index was shown to depend on the total runoff volume. It can be generalized that a higher total flood volume is linked to a lower baseflow index. Second, the copula parameter θ, was shown to depend on the event duration. A longer event duration is linked to a higher dependence between peak discharge and flood volume and therewith a higher θ value. Third, we showed that the shapes of shorter events, expressed by PDFs, generally show a steeper (lower scale parameter) and shorter (lower location parameter) rising limb than the shapes of longer events. The different characteristics of flood types in terms of their runoff behavior, their dependence between peak discharges and flood volumes, and their event shapes can be exploited by constructing flood type specific SDHs.

5.2. Flood type specific SDHs

The flood type specific peak discharges and flood volumes presented above show that the different flood types possess different hazard potentials. The severest floods in terms of flood volume are usually caused by LRFs independently of the size of the catchment. The flood volumes decrease from RoSFs to SRFs and FFs and are therefore linked to the

event duration. The reason for this is simply that more water becomes available to form runoff with increasing duration of the precipitation event. In terms of peak discharge, on the contrary, the severest floods not only depend on the flood type but also on the catchment size. In small catchments, peak discharges decrease from shorter events such as FFs and SRFs to longer lasting events such as RoSFs and LRFs. In contrast, the peak discharges in medium sized and large catchments were higher for longer lasting events and decrease with decreasing event duration. While intense rainfall causes a fast reaction in small catchments, it is locally restricted in larger catchments [*Grebner and Roesch*, 1998] and its effect is attenuated in larger catchments on the water's way to the outlet [*Maniak*, 2010]. Convective storms are therefore more effective in small basins than in large basins [*Sutcliffe*, 1998]. In larger catchments, longer lasting events, during which the hydrological condition of the soil changes, are of importance [*BWG*, 2005]. As soon as the soils are saturated, higher quantities of water will be available to form quick runoff. The hazard potential of a flood event is, besides the flood volume and the flood peak, also influenced by the shape of the design flood hydrograph [*Yue et al.*, 2002; *Mediero et al.*, 2010]. More storage volume is required to route a flood through a reservoir if the peak occurs early during an event than if the peak occurs later in the event. The catchment and flood type specific SDHs allow the practitioner to take account of these effects by providing information not only on flood peak and volume but also on the time of peak. The specific properties of the flood types regarding the flood hydrograph shape, design variables, and severity can help to find adequate flood protection strategies.

Knowledge on which flood type might cause the severest floods in the catchment of interest can be useful in flood prediction and flood risk management. Some of the flood

types have a pronounced seasonality and typically occur during certain seasons of the year. *Merz and Blöschl* [2003] found that in Austria, FFs mainly occur in summer and late summer while LRFs and SRFs have a less pronounced seasonality and RoSFs occur in periods when the temperature is around 0 C°. Our analysis confirms this general trend for floods in Switzerland. FFs mainly occurred in summer, LRFs mainly in winter and autumn, and SRFs all year round. If a flood risk manager knows that the catchment of interest is especially susceptible to FFs, he/she knows that the focus needs to lie on the prediction of floods caused by intense thunderstorms in summer. Flood type specific SDHs are not only helpful together with knowledge on the seasonality of occurrence but also together with the frequency of occurrence. Hydraulic structures can be laid out for the SDH of the severest and most frequent flood type in the catchment of interest. This is relevant to the practitioner because the choice of the design values directly influences the safety and the cost of a hydraulic structure [*Gräler et al.*, 2013]. The protection against the severest flood to be expected in a catchment can result in oversized structures that in turn can be cost-ineffective, ecologically disadvantageous, and negative for landscape value [*Perreault and Bobée*, 1998]. Considering not only one general catchment specific SDH but four flood type specific SDHs allows the practitioner to consider the severity of a flood jointly with the frequency of occurrence of the respective flood types. This might allow for a balance between sufficient protection and feasible costs.

5.3. Flood type specific SDHs for different return periods

We showed that the difference of SDHs for smaller and larger return periods depends on the bivariate distribution of peak discharges and flood volumes of the flood type analyzed. If the bivariate distribution has neither a bounded support for peaks nor volumes, a larger

return period results in both a higher peak discharge and a higher flood volume than a smaller return period. If, on the contrary, the distribution's support is bounded for the peaks, a larger return period does not lead to higher peaks than a smaller return period because higher values are not possible. The same is the case for the flood volumes if the distribution's support is bounded towards higher volumes. Whether a bivariate distribution is bounded in one or two directions depends partly on the flood type. Flood types characterized by a short duration, especially FFs, have generally little potential for the peak discharges or the flood volumes to move beyond certain values. This observation is closely linked to the classification procedure applied where FFs were defined as floods with a duration of less than six hours. The behavior of floods caused by rainfall of long duration is usually opposite of this. During an event with longer duration, the potential for higher peaks and especially higher flood volumes is given and the distribution can have a heavy upper tail. Despite the general pattern of more bounded distributions for event types with shorter duration and less bounded distributions for event types with longer distributions, the individual flood types have different bivariate distributions in different catchments. Therefore, the flood type specific SDHs of different return periods vary in the catchments analyzed. This indicates that the behavior of a flood is not only linked to the storm behavior and the precipitation input but also to the watershed and infiltration characteristics of a catchment [*Singh*, 1997].

5.4. Method evaluation

5.4.1. Application

The catchment specific SDH, where no differentiation is made between flood types, is usually similar to the SDH of the flood type observed most often in the catchment under

consideration. If the practitioner is interested in one single hydrograph estimate, he/she might therefore work with the catchment specific SDH. If he/she, however, wants to look at the spread of possible design events, the difference between the smallest and the largest flood type specific SDH can be considered. Taking into account the spread of possible events allows one to analyze not only events of the dominant flood type in a catchment but also events of flood types observed less frequently but potentially more hazardous. While the catchment specific SDH contains information on the frequency and on the magnitude of a flood event to be expected in a catchment, the flood type specific SDHs can also serve as an indicator for underlying processes. This approach satisfies the need for hydrological reasoning in the flood frequency estimation procedure as it was postulated by *Merz and Blöschl* [2008b]. The hydrological information content is not lost completely during the statistical estimation procedure but retained in the hydrograph shapes and design variable quantiles of the flood type specific SDHs. As it was already suggested by *Klemes* [1993], we tried to shed more light on the probabilities of hydrological extremes by incorporating more information on the physical basis of the phenomena and by increasing the homogeneity of the sample by splitting it into events belonging to different flood types [*Fischer et al.*, 2016]. The method can be applied to return periods of up to 100 years in gauged, medium sized catchments. The application to return periods higher than 100 years is highly discouraged because the reliability of a statistical statement is closely linked to the length of the observation period [*DVWK*, 1999]. The method allows for the use of different return period definitions, which need to be chosen according to the problem at hand [*Serinaldi*, 2015b; *Brunner et al.*, 2016], and is not restricted to the use of the joint OR return period used here.

Due to the limited sample size, it is desirable to not only communicate estimated design variable quantiles but to complement them with uncertainty bands. It was stressed by *Serinaldi* [2009] that the design variable quantiles have to be complemented with information about their uncertainty because they are provided for events whose frequency goes beyond the range that is supported by the length of the flood records [*Reed*, 2002]. In a bivariate framework, the uncertainty related to the limited sample size and the uncertainty of the marginal distributions combine with the uncertainty of the dependence structure between the two variables [*Serinaldi*, 2015b]. In our analysis, splitting the sample of flood events into subsamples for different flood types increases the uncertainty resulting from a limited sample size.

6. Conclusions and perspectives

In this study, we proposed a method that is not only suitable to construct catchment specific, but also flood type specific, synthetic design hydrographs (SDHs). The approach can not only be used when observed runoff data are available but also when the analyst is able to simulate synthetic discharge using continuous rainfall-runoff modelling. It relies on the fitting of probability density functions to observed flood hydrographs of a certain flood type taking into account the dependence between the design variables peak discharge and flood volume. The method makes use of the statistical information in the flood event data and retains some of the process based information stored in it. It thus helps to advance from a purely statistical method towards a method that incorporates more hydrological information. A flood type specific construction of SDHs is meaningful because flood types differ in their runoff behavior, their dependence between peak discharges and flood volumes, and their event shapes. Even though the method has been developed and tested

based on Swiss catchments, its applicability is not restricted to this geographical region but also extends to gauged catchments in other regions with similar catchments and data availability. So far, the approach is only applicable in gauged catchments with runoff and precipitation records but not in ungauged catchments. However, the estimation of design variables in ungauged catchments is of great interest [*Blöschl et al.*, 2013]. Therefore, the estimation of SDHs shall, in a next step, be regionalized to ungauged catchments where runoff data are not available. Further, the uncertainty introduced in each step of the method shall be assessed through a simulation study and the design variable estimates shall be complemented with uncertainty bands. We showed that flood type specific SDHs provide information not only on flood peak and volume but also on the time of peak and the whole event hydrograph for a certain flood type. They can be helpful in flood risk management together with knowledge on the seasonality and frequency of occurrence of different flood types.

Appendix A: Appendix I

Characteristics of 39 Swiss catchments used to develop and test the SDH construction approach (Table 3).

Acknowledgments. We thank the Federal Office for the Environment (FOEN) for funding the project (contract 13.0028.KP / M285-0623) and for providing runoff measurement data. We also thank MeteoSwiss for providing precipitation data. In addition, we thank Salvatore Grimaldi and the two anonymous reviewers for their constructive feedback, which helped to improve the quality of the paper. The data used in this study is available upon order from

the FOEN and MeteoSwiss. For the hydrological data, the order form under http://www.bafu.admin.ch/wasser/13462/13494/15076/index.html?lang=de can be used. The meteorological data can be ordered via https://shop.meteoswiss.ch/index.html.

References

Bhunya, P. K., R. Berndtsson, C. S. P. Ojha, and S. K. Mishra (2007), Suitability of Gamma, Chi-square, Weibull, and Beta distributions as synthetic unit hydrographs, *Journal of Hydrology*, *334*, 28–38.

Blöschl, G., M. Sivapalan, T. Wagener, A. Viglione, and H. Savenije (2013), *Runoff prediction in ungauged basins*, 465 pp., Cambridge University Press, Cambridge.

Boughton, W., and O. Droop (2003), Continuous simulation for design flood estimation - A review, *Environmental Modelling and Software*, *18*(4), 309–318, doi:10.1016/S1364-8152(03)00004-5.

Brunner, M. I., J. Seibert, and A.-C. Favre (2016), Bivariate return periods and their importance for flood peak and volume estimation, *Wire's Water*, *3*, 819–833, doi: 10.1002/wat2.1173.

BWG (2005), Hydrologie der Schweiz, *Tech. rep.*, Bundesamt für Wasser und Geologie, BWG.

Chernobai, A., S. T. Rachev, and F. J. Fabozzi (2015), Composite Goodness-of-Fit Tests for Left-Truncated Loss Samples, in *Handbook of financial econometrics and statistics*, edited by C.-F. Lee and J. Lee, chap. 20, pp. 575–596, Springer Science+Business Media, New York.

Coles, S. (2001), *An introduction to statistical modeling of extreme values*, 208 pp., Springer, London.

Cuevas, A., M. Febrero, and R. Fraiman (2007), Robust estimation and classification for functional data via projection-based depth notions, *Computational Statistics*, *22*(3), 481–496, doi:10.1007/s00180-007-0053-0.

Diezig, R., and R. Weingartner (2007), Hochwasserprozesstypen — Schlüssel zur Hochwasserabschätzung, *Wasser und Abfall*, *4*, 18–26.

DVWK (1999), Statistische Analyse von Hochwasserabflüssen, *Tech. rep.*, Deutscher Verband für Wasserwirtschaft, Bonn.

Eckhardt, K. (2005), How to construct recursive digital filters for baseflow separation, *Hydrological Processes*, *19*, 507–515.

Fischer, S., A. Schumann, and M. Schulte (2016), Characterisation of seasonal flood types according to timescales in mixed probability distributions, *Journal of Hydrology*, *539*, 38–56, doi:10.1016/j.jhydrol.2016.05.005.

Fraiman, R., and G. Muniz (2001), Trimmed means for functional data, *Test*, *10*(2), 419–440.

Gaal, L., J. Szolgay, S. Kohnova, K. Hlavcova, J. Parajka, A. Viglione, R. Merz, and G. Blöschl (2015), Dependence between flood peaks and volumes: a case study on climate and hydrological controls, *Hydrological Sciences Journal*, *60*(6).

Genest, C., and A.-C. Favre (2007), Everything you always wanted to know about copula modeling but were afraid to ask, *Journal of Hydrologic Engineering*, *12*(4), 347–367.

Genest, C., B. Rémillard, and D. Beaudoin (2009), Goodness-of-fit tests for copulas: A review and a power study, *Insurance: Mathematics and Economics*, *44*, 199–213.

Gonzales, a. L., J. Nonner, J. Heijkers, and S. Uhlenbrook (2009), Comparison of different base flow separation methods in a lowland catchment, *Hydrology and Earth System*

Sciences, *13*(11), 2055–2068, doi:10.5194/hess-13-2055-2009.

Gräler, B., M. J. van den Berg, S. Vandenberghe, A. Petroselli, S. Grimaldi, B. D. Baets, and N. E. C. Verhoest (2013), Multivariate return periods in hydrology: a critical and practical review on synthetic design hydrograph estimation, *Hydrological Earth System Sciences*, *17*, 1281–1296.

Grebner, D., and T. Roesch (1998), *Flächen-Mengen-Dauer Beziehungen von Starkniederschlägen und mögliche Niederschlagsgrenzwerte in der Schweiz*, 191 pp., Zürich.

Grimaldi, S., A. Petroselli, G. Salvadori, and C. De Michele (2016), Catchment compatibility via copulas: A non-parametric study of the dependence structures of hydrological responses, *Advances in Water Resources*, *90*, 116–133, doi: 10.1016/j.advwatres.2016.02.003.

Gupta, H. V., H. Kling, K. K. Yilmaz, and G. F. Martinez (2009), Decomposition of the mean squared error and NSE performance criteria: Implications for improving hydrological modelling, *Journal of Hydrology*, *377*, 80–91.

Hao, Z., and V. P. Singh (2016), Review of dependence modeling in hydrology and water resources, *Progress in Physical Geography*, *40*(4), 549–578, doi: 10.1177/0309133316632460.

Heffernan, J. E. (2000), A Directory of Coeffcients of Tail Dependence, *Extremes*, *33*, 279–290.

Hofert, M., M. Mächler, and A. J. McNeil (2012), Likelihood inference for Archimedean copulas in high dimensions under known margins, *Journal of Multivariate Analysis*, *110*, 133–150, doi:10.1016/j.jmva.2012.02.019.

Joe, H. (2014), *Dependence modeling with copulas.*, 480 pp., Chapman & Hall/CRC.

Klein, B., M. Pahlow, Y. Hundecha, and A. Schumann (2010), Probability analysis of hydrological loads for the design of flood control systems using copulas, *Journal of Hydrologic Engineering*, *15*(5), doi:10.1061/(ASCE)HE.1943-5584.0000204.

Klemes, V. (1993), Probability of extreme hydrometeorological events - a different approach, *IAHS*, *213*, 167–176.

Klemes, V. (2000), Tall tales about tails of hydrological distributions I, *Journal of Hydrologic Engineering*, *5*(3), 227–231.

Lang, M., T. Ouarda, and B. Bobée (1999), Towards operational guidelines for over-threshold modeling, *Journal of Hydrology*, *225*, 103–117.

López-Pintado, S., and J. Romo (2009), On the Concept of Depth for Functional Data, *Journal of the American Statistical Association*, *104*, 718–734, doi: 10.1198/jasa.2009.0108.

Maniak, U. (2010), *Hydrologie und Wasserwirtschaft. Eine Einführung für Ingenieure*, 686 pp., Springer-Verlag, Berlin-Heidelberg.

Mathevet, T., C. Michel, V. Andréassian, and C. Perrin (2006), A bounded version of the Nash-Sutcliffe criterion for better model assessment on large sets of basins, *IAHS*, *307*, 211–219.

Mediero, L., A. Jiménez-Alvarez, and L. Garrote (2010), Design flood hydrographs from the relationship between flood peak and volume, *Hydrological Earth System Sciences*, *14*, 2495–2505.

Mengersen, K., C. Robert, and D. M. Titterington (2011), *Mixtures: Estimation and applications*, 1st ed., 330 pp., John Wiley & Sons Ltd, Chichester (UK).

Merz, B., et al. (2014), Floods and climate: emerging perspectives for flood risk assessment and management, *Natural Hazards and Earth System Science*, *14*(7), 1921–1942.

Merz, R., and G. Blöschl (2003), A process typology of regional floods, *Water resources research*, *39*(12), 1340, doi:10.1029/2002WR001952.

Merz, R., and G. Blöschl (2008a), Flood frequency hydrology: 1. Temporal, spatial, and causal expansion of information, *Water Resources Research*, *44*, doi:10.1029/2007WR006744.

Merz, R., and G. Blöschl (2008b), Flood frequency hydrology: 2. Combining data evidence, *Water Resources Research*, *44*, doi:10.1029/2007WR006745.

Meyer, R., B. Schädler, D. Viviroli, and R. Weingartner (2011), Die Rolle des Basisabflusses bei der Modellierung von Niedrigwasserprozessen in Klimaimpaktstudien, *Hydrologie und Wasserbewirtschaftung*, *55*, 244–257.

Nadarajah, S. (2007), Probability models for unit hydrograph derivation, *Journal of Hydrology*, *344*, 185–189.

Nelsen, R. B. (2005), *An introduction to copulas*, 2nd ed., 269 pp., Springer Science & Business Media, New York.

Pathiraja, S., S. Westra, and A. Sharma (2012), Why continuous simulation? the role of antecedent moisture in design flood estimation, *Water Resources Research*, *48*(6), 1–15, doi:10.1029/2011WR010997.

Perreault, L., and B. Bobée (1998), Modélisation de données hydrologiques extrêmes de crues à l'aide des lois de Halphen, in *Statistical and Bayesian methods in hydrological sciences*, edited by E. Parent, P. Hubert, B. Bobée, and J. Miquel, pp. 87–106, UNESCO, Paris.

Pilgrim, D. H., and I. Cordery (1993), Flood runoff, in *Handbook of hydrology*, edited by D. R. Maidment, chap. 9, pp. 477–546, McGraw-Hill.

Rai, R. K., S. Sarkar, and V. P. Singh (2009), Evaluation of the adequacy of statistical distribution functions for deriving unit hydrograph, *Water Resources Management*, *23*, 899–929.

Ramirez, J. A. (2000), Prediction and modeling of flood hydrology and hydraulics, in *Inland flood hazards: Human riparian and aquatic communities*, edited by E. Wohl, p. 53, Cambridge University Press.

Ramsay, J. O., and B. W. Silverman (2002), *Applied functional data analysis: methods and case studies*, 190 pp., doi:10.1007/b98886.

Reed, D. W. (2002), Reinforcing flood-risk estimation, *Philosophical Transactions of the Royal Society of London*, *360*, 1373–1387.

Rickenmann, D. (1997), Sediment transport in Swiss torrents, *Earth surface processes and landforms*, *22*(10), 937–951.

Rogger, M., B. Kohl, H. Pirkl, A. Viglione, J. Komma, R. Kirnbauer, R. Merz, and G. Blöschl (2012), Runoff models and flood frequency statistics for design flood estimation in Austria — Do they tell a consistent story?, *Journal of Hydrology*, *456*, 30–43, doi:10.1016/j.jhydrol.2012.05.068.

Rosbjerg, D., et al. (2013), Prediction of floods in ungauged basins, in *Runoff prediction in ungauged basins. A synthesis across processes, places and scales*, edited by G. Blöschl, M. Sivapalan, T. Wagener, A. Viglione, and H. Savenije, chap. 9, pp. 189–226, Cambridge University Press, Cambridge.

Salvadori, G., C. DeMichele, and F. Durante (2011), On the return period and design in a multivariate framework, *Hydrological Earth System Sciences*, *15*, 3293–3305.

Schreider, S. Y., P. H. Whetton, A. J. Jakeman, and A. B. Pittok (1997), Runoff modelling for snow-affected catchments in the Australian alpine region, eastern Victoria, *Journal of Hydrology*, *200*, 1–23.

Seibert, J. (1999), Regionalisation of parameters for a conceptual rainfall-runoff model, *Agricultural and Forest Meteorology*, *98-99*, 279–293.

Serinaldi, F. (2009), Assessing the applicability of fractional order statistics for computing confidence intervals for extreme quantiles, *Journal of Hydrology*, *376*, 528–541.

Serinaldi, F. (2015a), Dismissing return periods!, *Stochastic Environmental Research and Risk Assessment*, *29*, 1179–1189.

Serinaldi, F. (2015b), Can we tell more than we can know? The limits of bivariate drought analyses in the United States, *Stochastic Environmental Research and Risk Assessment*, pp. 1–14.

Serinaldi, F., and S. Grimaldi (2011), Synthetic design hydrographs based on distribution functions with finite support, *Journal of Hydrologic Engineering*, *16*, 434–446.

Serinaldi, F., and C. Kilsby (2013), The intrinsic dependence structure of peak, volume, duration, and average intensity of hyetographs and hydrographs, *Water Resources Research*, *49*, 3424–3442.

Sikorska, A. E., D. Viviroli, and J. Seibert (2015), Flood type classification in mountainous catchments using crisp and fuzzy decision trees, *Water Resources Research*, *51*(10), 7959–7976, doi:10.1002/2015WR017326.

Singh, V. P. (1997), Effect of spatial and temporal variability in rainfall and watershed characteristics on stream flow hydrograph, *Hydrological processes*, *11*, 1649–1669.

Smakhtin, V. U. (2001), Low flow hydrology: a review, *Journal of Hydrology*, *240*, 147–186.

Smakhtin, V. Y., and B. Masse (2000), Continuous daily hydrograph simulation using duration curves of a precipitation index, *Hydrological Processes*, *14*, 1083–1100.

Smithers, J. C. (2012), Methods for design flood estimation in South Africa.

Sutcliffe, J. V. (1998), Flood frequency studies using regional methods, in *Statistical and Bayesian methods in hydrological sciences*, edited by E. Parent, P. Hubert, B. Bobée, and J. Miquel, pp. 341–355, UNESCO, Paris.

Szolgay, J., L. Gaal, S. Kohnova, K. Hlavcova, R. Vyleta, T. Bacigal, and G. Blöschl (2015), A process-based analysis of the suitability of copula types for peak-volume flood relationships, in *Proceedings of the International Association of Hydrological Sciences*, pp. 183–188, IAHS, doi:10.5194/piahs-370-183-2015.

Tanaka, S., and K. Takara (2002), A study on threshold selection in POT analysis of extreme floods, *IAHS publications: The Extremes of the Extremes: Extraordinary Flood*, (271), 299–304.

Viglione, a., R. Merz, and G. Blöschl (2009), On the role of the runoff coefficient in the mapping of rainfall to flood return periods, *Hydrology and Earth System Sciences Discussions*, *6*(1), 627–665, doi:10.5194/hessd-6-627-2009.

Viviroli, D., and R. Weingartner (2004), The hydrological significance of mountains: from regional to global scale, *Hydrology & Earth System Sciences*, *8*(6), 1016–1029.

Xiao, Y., S. Guo, P. Liu, B. Yan, and L. Chen (2009), Design flood hydrograph based on multicharacteristic synthesis index method, *Journal of Hydrologic Engineering*, *14*(12), 1359–1364.

Yue, S., T. Ouarda, B. Bobée, P. Legendre, and P. Bruneau (2002), Approach for describing statistical properties of flood hydrograph, *Journal of Hydrologic Engineering*, *7*(2), 147–153.

Figure 1. Map of the 39 catchments used for developing and testing the method for constructing flood type specific SDHs. The three catchments used to illustrate flood type specific SDHs are highlighted in green and the remaining 36 catchments in brown. The gauging stations are indicated as red crosses and labelled with the catchment ID given in Table 3.

Table 1. Overview of the minimum, first quartile, median, third quartile, and maximum of the distribution of the following catchment characteristics for the 39 study catchments: record length [years], catchment area [km^2], station elevation [m.a.s.l.], mean catchment elevation [m.a.s.l.], glacier cover [%], maximum peak discharge observed in the catchment [m^3/s], maximum specific peak discharge [$l/(s \cdot km^2)$], maximum flood volume observed in the catchment [m^3], and maximum specific flood volume observed in the catchment [$10^3 \cdot m^3/km^2$].

Catchment characteristics	Minimum	First quartile	Median	Third quartile	Maximum
Record length [years]	17	34	40	40	53
Catchment area [km^2]	22	60	119	347	1696
Station elevation [m.a.s.l.]	247	403	511	654	1707
Mean elevation [m.a.s.l.]	370	718	930	1129	2450
Glacier cover [%]	0	0	0	0	14
Maximum peak discharge [m^3/s]	11	62	122	276	956
Maximum specific peak discharge [$l/(s \cdot km^2)$]	191	634	947	1468	3123
Maximum flood volume [m^3]	234	993	1918	4503	27397
Maximum specific flood volume [$10^3 \cdot m^3/km^2$]	85	2728	4197	6825	35690

Figure 2. Method developed to construct synthetic design hydrographs (SDHs) for catchments in Switzerland. The method can either be applied to all types of flood events identified in a catchment or it can be used to construct flood type specific SDHs. Flood type specific SDHs can be constructed for flash floods (FF), short-rain floods (SRF), long-rain floods (LRF), or rain-on-snow floods (RoSF), but not for snowmelt floods (SMF) and glaciermelt floods (GMF). The approach consists of eleven steps whose numbers correspond to the section numbers in the Methods chapter. The SDH ($Q_T(t)$) can be expressed by a probability density function ($f(t)$) times the mean discharge (V_T/D_T) plus the baseflow (B).

Figure 3. Frequency and seasonality of the six flood types obtained by the classification procedure: flash floods (FFs), short-rain floods (SRFs), long-rain floods (LRFs), rain-on-snow floods (RoSFs), snowmelt floods (SMFs), and glacier melt floods (GMFs) over the 39 study catchments. The seasons were defined as follows: winter: December-February; spring: March-May; summer: June-August; autumn: September-November.

Table 2. Overview on the minimum, first quartile, median, mean, third quartile, and maximum of the number of events per flood type over the 39 test catchments (the numbers were rounded to integers).

Flood type	Minimum	First quartile	Median	Mean	Third quartile	Maximum
FF	4	15	19	24	34	59
SRF	33	48	64	61	70	86
LRF	5	10	13	16	20	45
RoSF	3	8	14	16	20	60
SMF	0	1	2	3	4	12
GMF	0	0	0	0	0	10

Figure 4. Four selected SDH parameters per flood type. a) baseflow index (I_{BF}), (b) copula parameter θ, (c) location parameter of the probability distribution function Lognormal (PDF location), (d) scale parameter of the probability distribution function Lognormal (PDF scale).

Figure 5. Flood type specific SDHs for three catchments of the same mean elevation zone (650-800 m.a.s.l.) but different sizes (a) Langete at Huttwil: 60 km^2; b) Mentue at Yvonand: 105 km^2; c) Birs at Münchenstein: 911 km^2. The duration is centered around the time of occurrence of the peak which was set to zero and therefore the time is negative before and positive after the peak. The line width of the SDH represents the frequency of occurrence of a certain type in the respective catchment. The highest observed event in the catchment is shown in black.

Figure 6. Flood type specific design variables per catchment size group: a) specific peak discharges [l/(s·km^2)], b) specific flood volumes [$10^3\cdot$ m^3/km^2]. The size of small catchments ranges from 20-75 km^2, that of medium catchments from 76-300 km^2, and that of large catchments from 301-1700 km^2. The different flood types are represented by different colors.

Figure 7. SDHs for Mentue at Yvonand for three different return periods T = 20, 50, 100 years for return periods defined after the joint OR probability approach for the different flood types and over all types. The joint OR probability refers to the probability that either the peak discharge, or the volume, or both, exceed a certain value. a) Flood type specific SDHs for different return periods. b) Flood type specific design variable quantiles for different return periods. c) Random sample of the bivariate distribution of peak discharges and flood volumes for the different flood types and over all flood types.

Table 3. Characteristics of 39 Swiss catchments used to develop and test the SDH construction approach.

ID	River	Gauging station	Area [km^2]	Station elevation [m.a.s.l.]	Mean elevation [m.a.s.l.]	Degree of glaciation [%]	Record length [years]
1	Aach	Salmsach, Hungerbühl	49	406	480	0	40
2	Allenbach	Adelboden	29	1297	1856	0	40
3	Allondon	Dardagny, Les Granges	119	400	758	0	29
4	Bibere	Kerzers	50	443	540	0	34
5	Birse	Moutier, La Charrue	183	519	930	0	40
6	Birs	Münchenstein, Hofmatt	911	268	726	0	40
7	Breggia	Chiasso, Ponte di Polenta	47	255	927	0	40
8	Broye	Payerne, Caserne d'aviation	392	441	710	0	40
9	Cassarate	Pregassona	74	291	990	0	40
10	Emme	Eggiwil, Heidbüel	124	745	1189	0	39
11	Emme	Emmenmatt	443	638	1070	0	17
12	Emme	Wiler, Limpachmündung	939	458	860	0	40
13	Ergolz	Liestal	261	305	590	0	40
14	Goldach	Goldach, Bleiche	50	399	833	0	23
15	Goneri	Oberwald	40	1385	2377	14	23
16	Gürbe	Belp	117	511	837	0	40
17	Ilfis	Langnau	188	685	1051	0	25
18	Kleine Emme	Littau, Reussbühl	477	431	1050	0	36
19	Kleine Emme	Werthenstein, Chappelboden	311	540	1173	0	30
20	Langeten	Huttwil, Häberenbad	60	597	766	0	40
21	Mentue	Yvonand, La Mauguettaz	105	449	679	0	40
22	Minster	Euthal, Rüti	59	894	1351	0	40
23	Murg	Frauenfeld	212	390	580	0	40
24	Murg	Wängi	79	466	650	0	40
25	Necker	Mogelsberg, Aachsäge	88	606	959	0	40
26	Ova dal Fuorn	Zernez, Punt la Drossa	55	1707	2331	0	40
27	Plessur	Chur	263	573	1850	0	40
28	Sense	Thörishaus, Sensematt	352	555	1068	0	36
29	Somvixer Rhein	Somvix, Encardens	22	1490	2450	7	36
30	Steinach	Steinach, Mattenhof	24	406	710	0	30
31	Suze	Sonceboz	150	642	1050	0	53
32	Taschinasbach	Grüsch, Wasserfassung Lietha	63	666	1768	0	34
33	Thur	Andelfingen	1696	356	770	0	40
34	Thur	Halden	1085	456	910	0	40
35	Thur	Jonschwil, Mühlau	493	534	1030	0	40
36	Thur	Stein, Iltishag	84	850	1448	0	31
37	Töss	Neftenbach	342	389	650	0	40
38	Urnäsch	Hundwil, Äschentobel	65	746	1085	0	33
39	Wiese	Basel	437	247	370	0	40

Figure 1. Figure

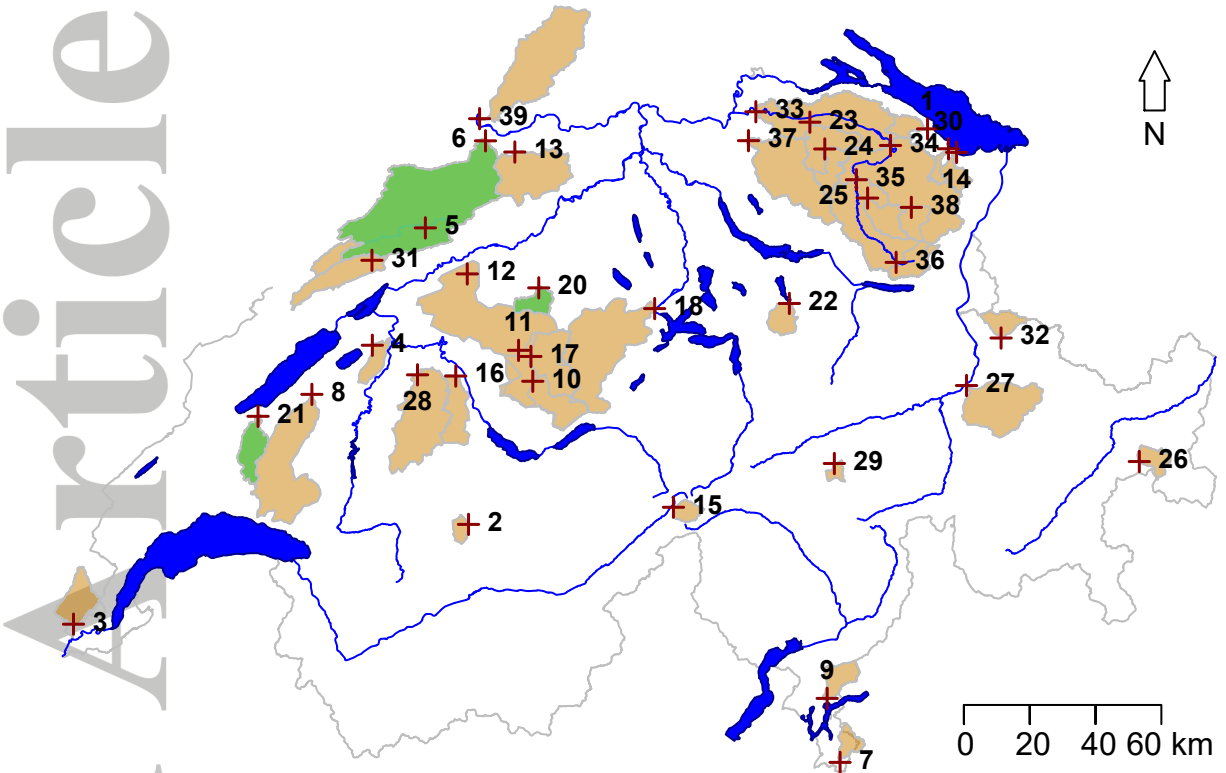

Figure 2. Figure

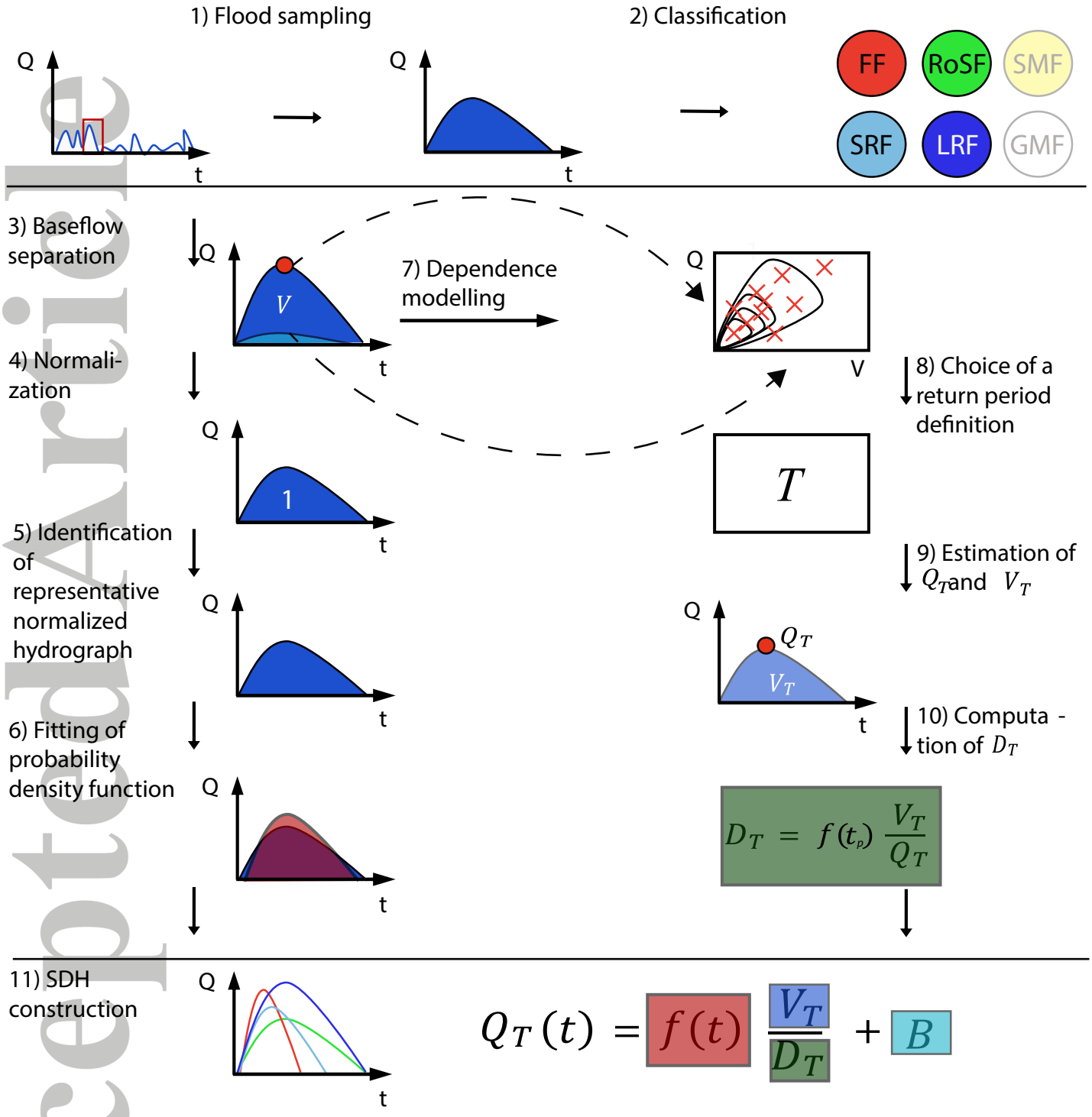

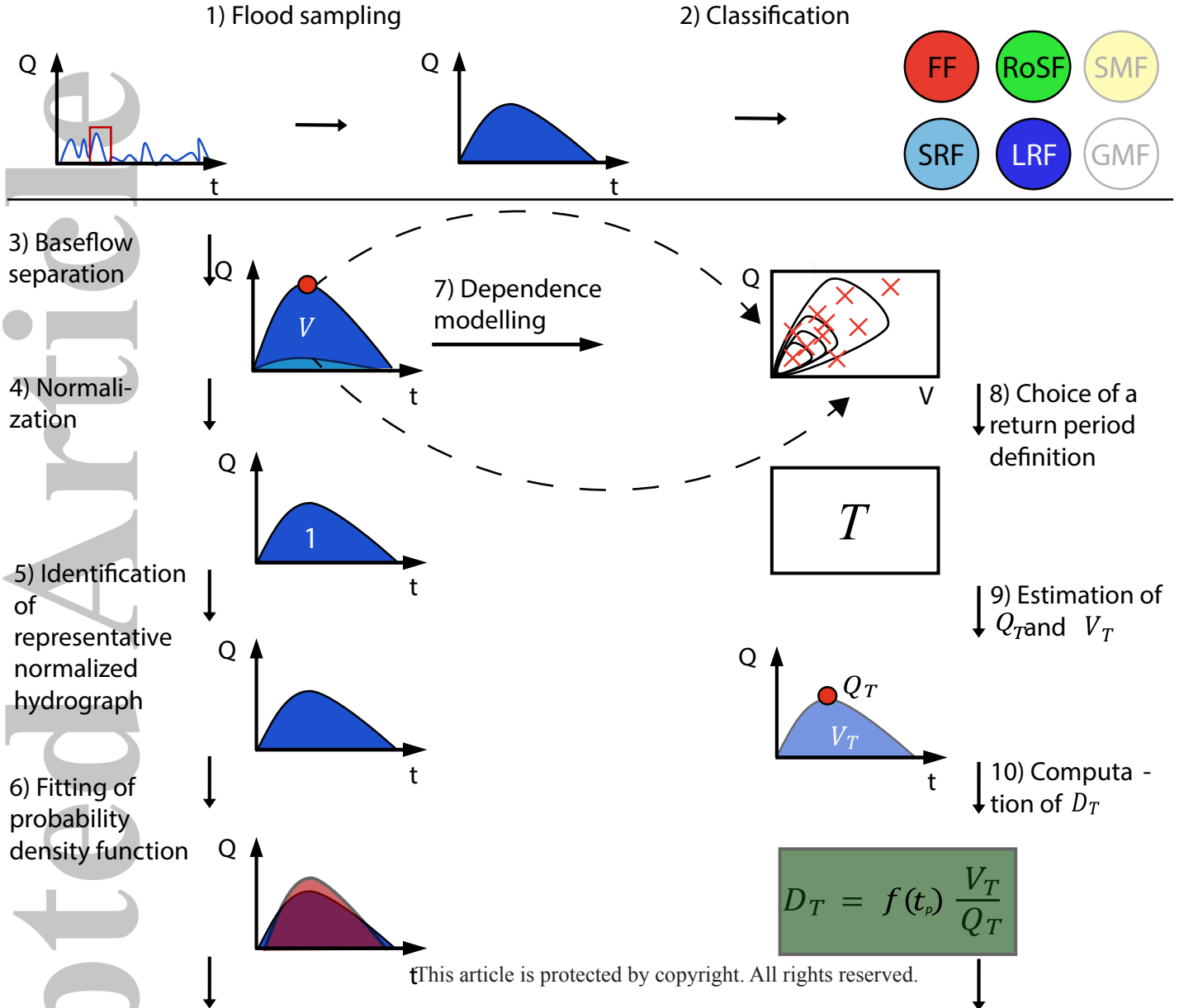

Figure 3. Figure

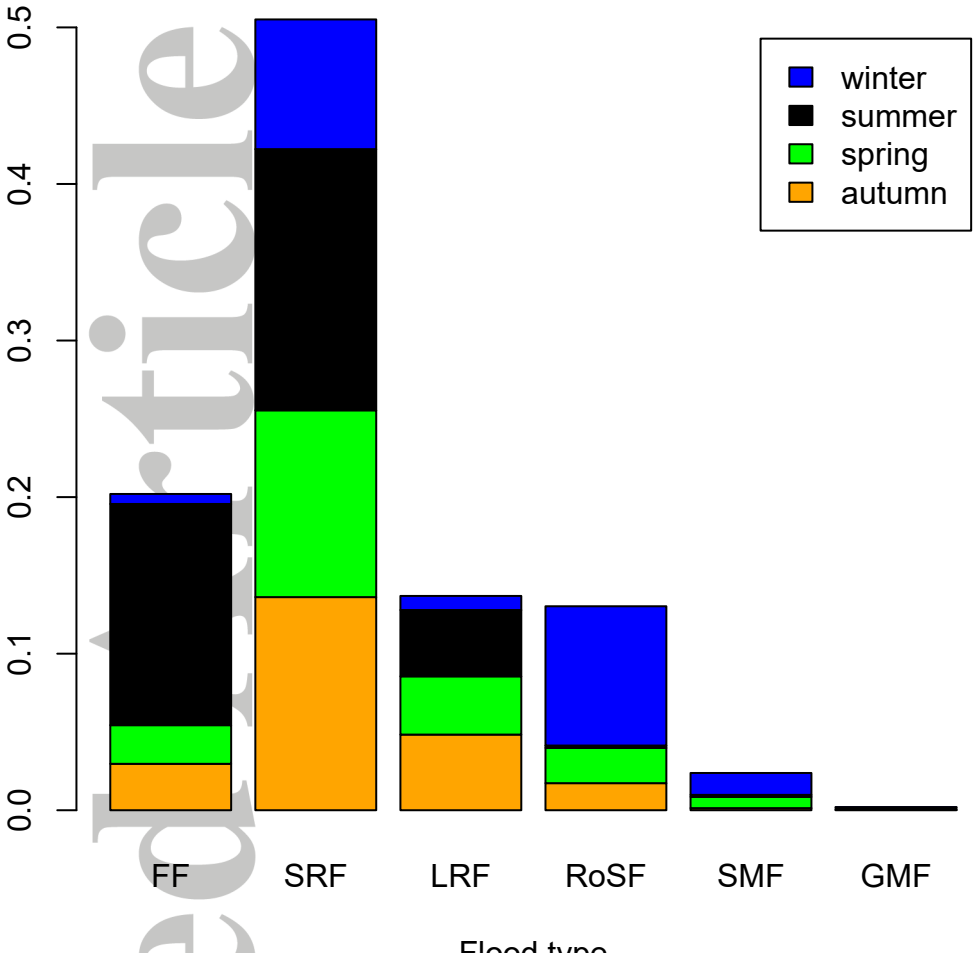

Figure 4.

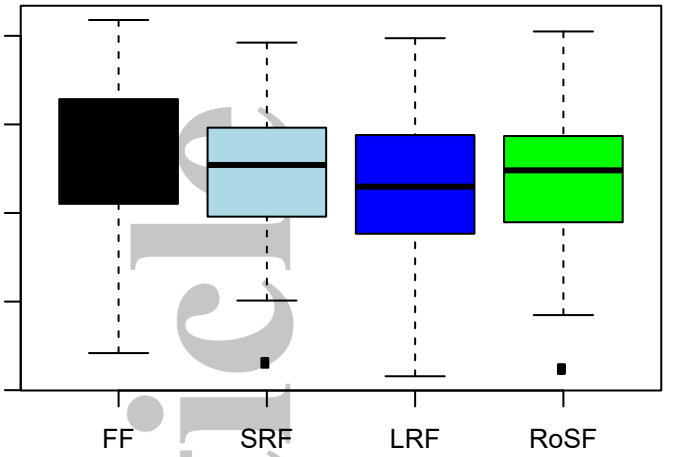

a) I_{BF}

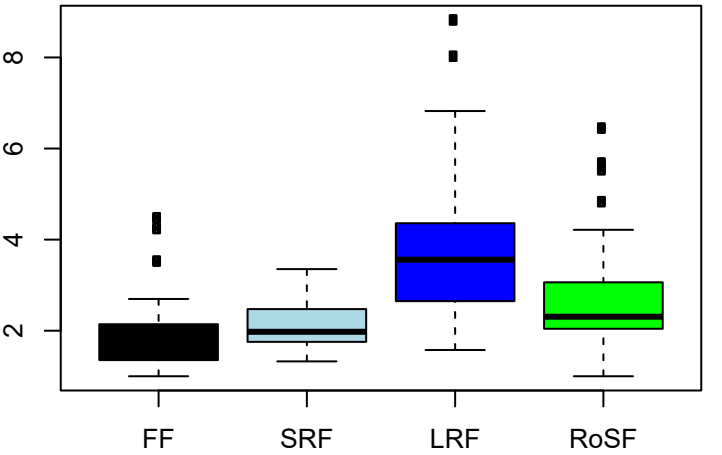

b) θ

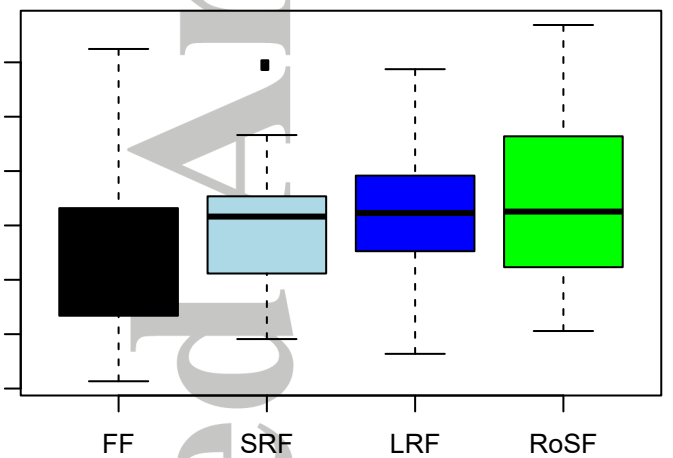

c) PDF location

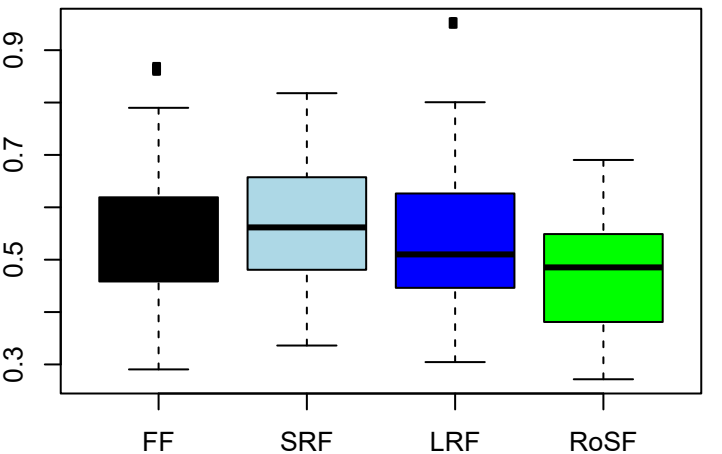

d) PDF scale

Figure 5.

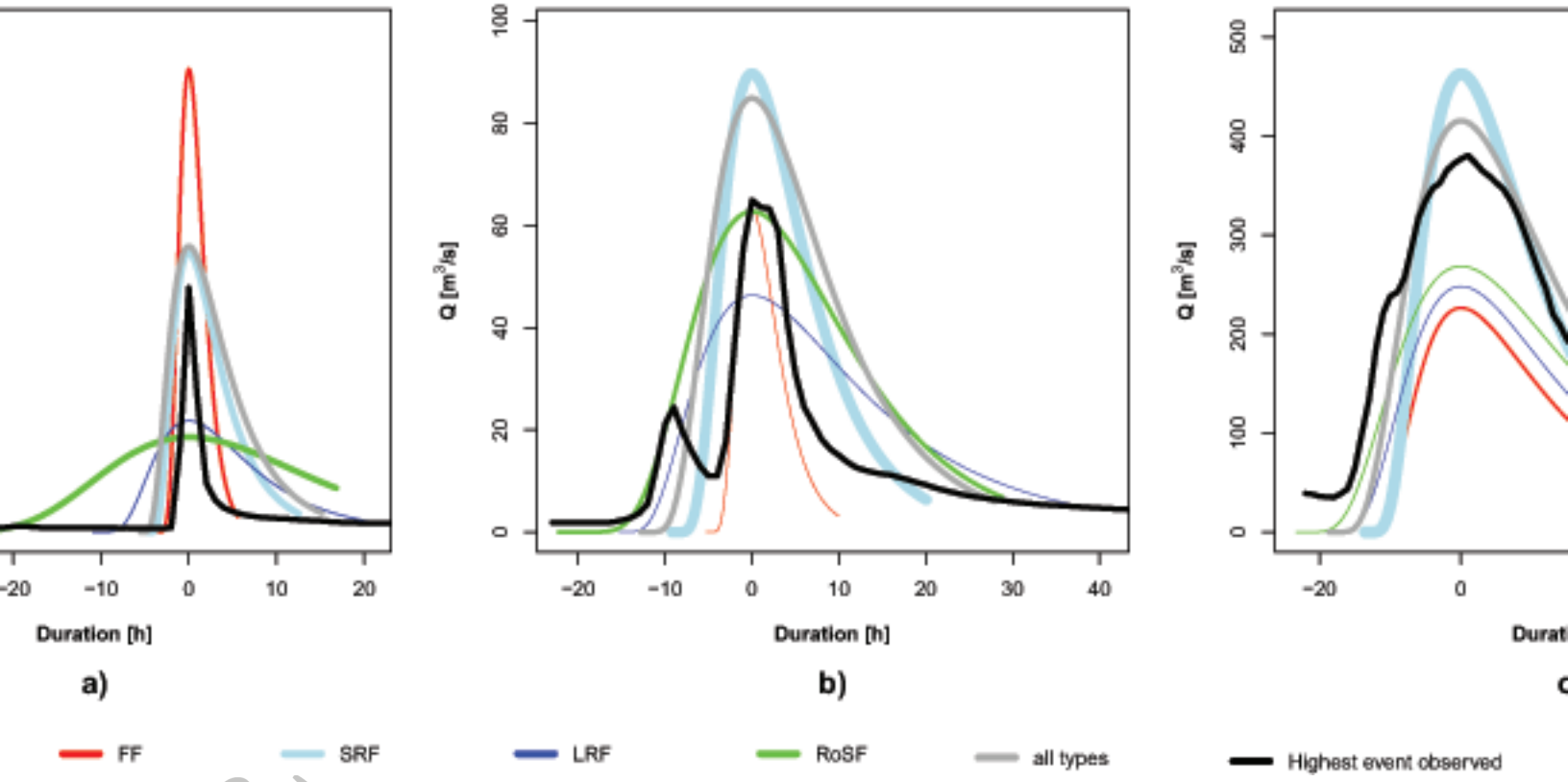

Figure 6. Figure

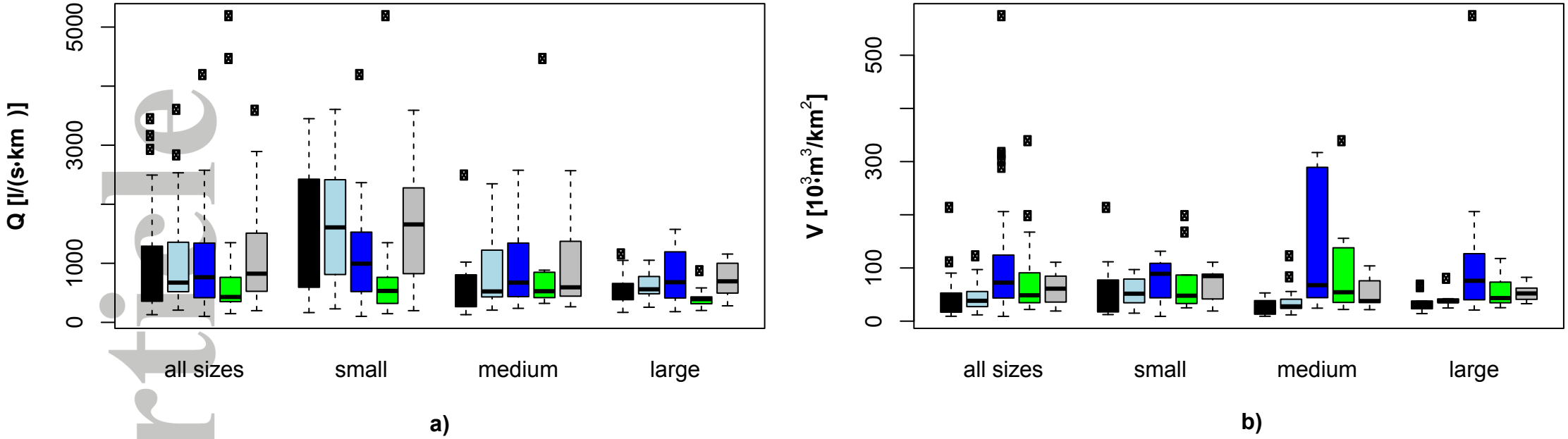

Figure 7.

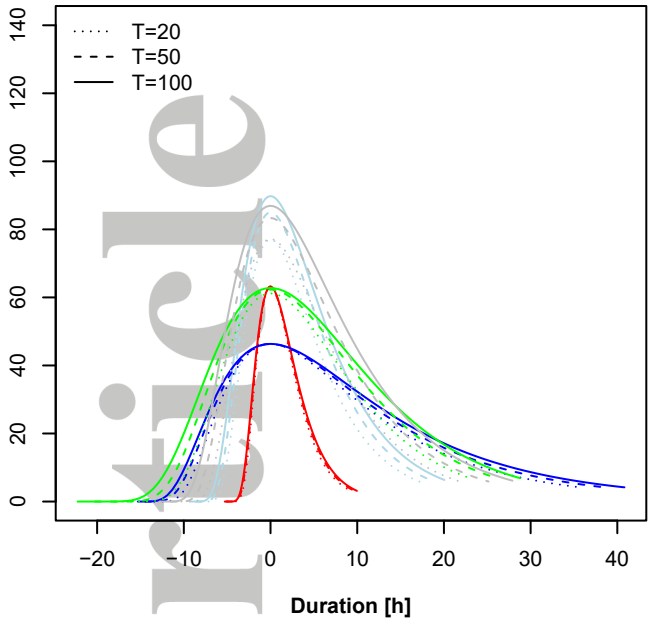

a)

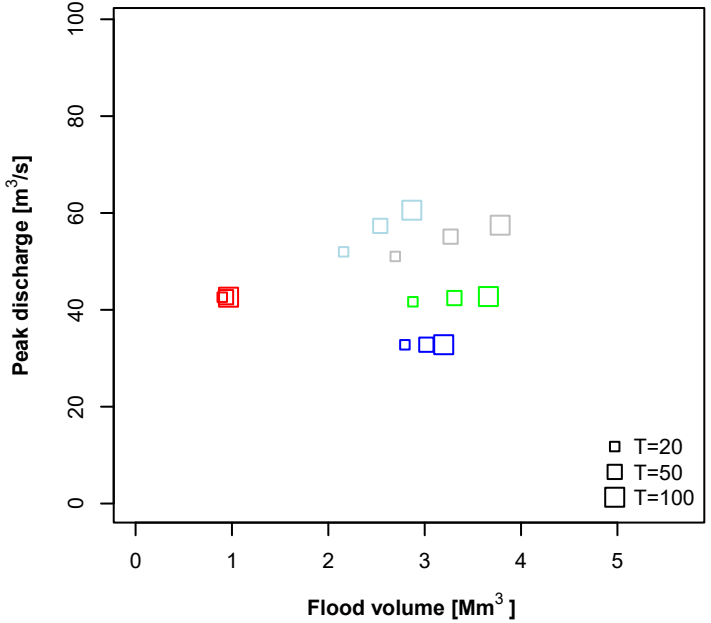

b)

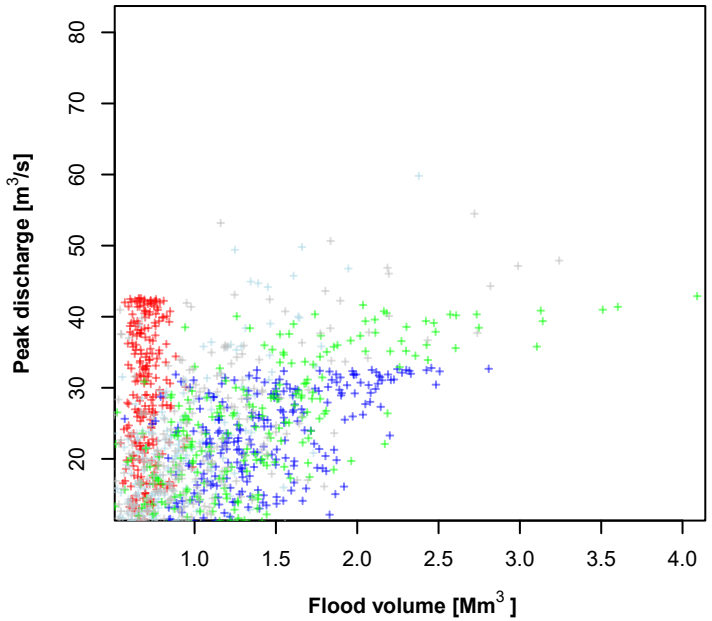

c)